

Conformational Properties of Ethyl- and 2,2,2-Trifluoroethyl Thionitrites, (CXCHSNO, X = H and F)

Antonela Cánneva, Carlos Omar Della Védova, Norbert Werner Mitzel, and Mauricio Federico Erben

J. Phys. Chem. A, **Just Accepted Manuscript** • Publication Date (Web): 04 Sep 2014

Downloaded from <http://pubs.acs.org> on September 4, 2014

Just Accepted

“Just Accepted” manuscripts have been peer-reviewed and accepted for publication. They are posted online prior to technical editing, formatting for publication and author proofing. The American Chemical Society provides “Just Accepted” as a free service to the research community to expedite the dissemination of scientific material as soon as possible after acceptance. “Just Accepted” manuscripts appear in full in PDF format accompanied by an HTML abstract. “Just Accepted” manuscripts have been fully peer reviewed, but should not be considered the official version of record. They are accessible to all readers and citable by the Digital Object Identifier (DOI®). “Just Accepted” is an optional service offered to authors. Therefore, the “Just Accepted” Web site may not include all articles that will be published in the journal. After a manuscript is technically edited and formatted, it will be removed from the “Just Accepted” Web site and published as an ASAP article. Note that technical editing may introduce minor changes to the manuscript text and/or graphics which could affect content, and all legal disclaimers and ethical guidelines that apply to the journal pertain. ACS cannot be held responsible for errors or consequences arising from the use of information contained in these “Just Accepted” manuscripts.



1
2
3 **Conformational Properties of Ethyl- and 2,2,2-Trifluoroethyl**
4
5 **Thionitrites, (CX₃CH₂SNO, X = H and F)**
6
7
8
9
10

11 Antonela Cánneva,^a Carlos O. Della Védova^{a,*}, Norbert W. Mitzel,^b and Mauricio F.
12 Erben^{a,*}
13
14
15
16
17
18
19

20 ^a *CEQUINOR (UNLP-CONICET, CCT, La Plata), Departamento de Química, Facultad*
21 *de Ciencias Exactas, Universidad Nacional de La Plata, CC962, La Plata (CP 1900),*
22 *República Argentina*
23
24
25
26

27 ^b *Universität Bielefeld, Lehrstuhl für Anorganische Chemie und Strukturchemie,*
28 *Centrum für Molekulare Materialien CM₂, Universitätsstraße 25, 33615 Bielefeld,*
29 *Germany.*
30
31
32
33
34
35
36
37
38
39
40
41
42
43
44
45
46
47
48
49
50
51
52

53 * Corresponding authors: Tel/Fax: ++54-221-425-9485, E-mail: erben@quimica.unlp.edu.ar
54 (MFE), carlosdv@quimica.unlp.edu.ar (CODV).
55
56
57
58
59
60

Abstract

The simple 2,2,2-trifluoroethyl thionitrite molecule, $\text{CF}_3\text{CH}_2\text{SNO}$, has been prepared in good yield for the first time using $\text{CF}_3\text{CH}_2\text{SH}$ and NOCl in slight excess. The vapor pressure of the red-brown compound $\text{CF}_3\text{CH}_2\text{SNO}$ follows, in the temperature range between 226 and 268 K, the equation $\log p = 12.0 - 3881/T$ (p/bar , T/K), and its extrapolated boiling point reaches 51 °C. Its structural and conformational properties have been compared with the ethyl thionitrite analogue, $\text{CH}_3\text{CH}_2\text{SNO}$. The FTIR spectra of the vapor of both thionitrites show the presence of bands with well-defined contours, allowing for a detailed conformational analysis and vibrational assignment on the basis of a normal coordinate analysis. The conformational space of both thionitrite derivatives has also been studied by using the DFT and MP2(full) level of theory with extended basis sets [6-311+G(2df) and cc-pVTZ]. The overall evaluation of the experimental and theoretical results suggests the existence of a mixture of two conformers at room temperature. The relative abundance of the most stable syn form (N=O double bond syn with respect to the C–S single bond) has been estimated to be ca. 79 and 75 % for $\text{CF}_3\text{CH}_2\text{SNO}$ and $\text{CH}_3\text{CH}_2\text{SNO}$, respectively.

Keywords: S-nitrosothiol, Conformational analysis, IR Spectroscopy, Vibrational properties, Molecular structure.

1-Introduction

The first preparation of an *S*-nitrosophenylthiol species by reacting benzenethiol and nitrosyl chloride was reported more than a century ago by Tasker and Jones.¹ Different synthetic methods for thionitrites RSNO, are currently available in the chemical literature,²⁻⁴ which includes outstanding reviews on its chemistry.⁵ Mainly due to their thermal and photochemical instability, this family of compounds remained scarcely studied until recent times, when the formation and decomposition of RSNOs have been suggested as a mechanism for the storage and delivering of nitric oxide (NO) within the mammalian body.⁶⁻⁹ Since then, a series of works have been reported in the literature, focusing on the study of fundamental properties of the simpler representatives, typically with R = alkyl or aryl groups.¹⁰⁻¹⁴

In this context, the first molecular structure experimentally determined for a thionitrite compound – *S*-nitroso-*N*-acetyl-D,L-penicillamine – was reported in 1978 by the Carnahan group.^{15,16} The molecular structure of tri-phenyl thionitrite in the crystalline state determined by X-ray diffraction was reported in 1999 by Arulsami et al.¹⁷ This structure shows an *anti* conformation [$\tau(\text{CS-NO})=175.7^\circ$], with bond lengths of 1.792(5) and 1.177(6) Å for the S–N and N=O bonds, respectively.¹⁷ On the other hand, the *syn* conformation [$\tau(\text{CS-NO})= 0.7^\circ$] was observed in the crystal structure of *S*-nitrosocaptopril, which can deliver NO and captopril under physiological conditions, with S–N and N=O bond lengths of 1.766 and 1.206 Å, respectively.^{18,19} Few other experimentally determined structures can be found in the literature.¹⁹⁻²¹ In general it was assumed that – mainly due to sterical reasons – tertiary thionitrites prefer the *anti* conformation, whereas the *syn* form is adopted by primary derivatives. However, a delicate balance between both steric and electronic effects are known to affect the conformational behavior.²² Moreover, for compounds containing a bond isomer with –

1
2
3 N=S=O unit it was also the case. The structure of PhNSO is planar and the introduction
4
5 of two bulky ethyl groups in *ortho* positions does not change the transferable *syn* R–
6
7 N=S=O configuration but rotate the –N=S=O group by 55.3° from a planar
8
9 arrangement.²³
10

11
12 For the “parent” HSNO species, benchmarking calculations suggest that the *anti*
13
14 conformation is more stable than the *syn* one by 0.74 kcal/mol [CCSD(T)/AVQZ
15
16 including corrections for core valence and scalar-relativistic and spin orbit effects]^{13,24}
17
18 in very good agreement with recent calculations performed at the explicitly correlated
19
20 coupled cluster approach (RCCSD(T)-F12) in connection with the cc-pVTZ-F12 basis
21
22 set, that provides an accurate $\Delta E = 0.715$ kcal/mol.²⁵
23
24
25

26
27 Furthermore, on the basis of spectroscopic studies, it is well-known that the
28
29 simplest alkylated derivative, methyl thionitrite (CH₃SNO), is present as a mixture of
30
31 two conformers in the gas phase, with the *syn* conformer being the most abundant
32
33 one.²⁶⁻²⁹ By irradiating with visible light (between 485 and 590 nm) the mixture of both
34
35 conformers isolated in a Ar matrix at 12 K, Müller and Huber determined a $\Delta G^\circ_{298} =$
36
37 1.33 ± 0.18 kcal/mol for the *syn* ⇌ *anti* equilibrium.³⁰ These conformational properties
38
39 were also confirmed in the photodissociation dynamics of jet-cooled CH₃SNO using
40
41 355 nm polarized laser photolysis.³¹
42
43
44

45
46 It was reported for the related alkyl nitroso compounds, RONO,^{32,33} that the
47
48 perfluorination of the alkyl group leads to a stabilization of the labile functional group,²⁸
49
50 but this seems not to be the case for RSNO compounds, in which the stability appears to
51
52 decrease with increasing electron-withdrawing effect of R. To the best of our
53
54 knowledge, the only known fluorinated thionitrite, CF₃SNO, was prepared by Mason in
55
56 1969 and its infrared and UV-vis spectra in the gas phase were interpreted in terms “*of a*
57
58
59
60

1
2
3 *molecule of C_s symmetry, probably trans*".³⁴ This preference for the *anti* conformer was
4
5 recently confirmed by quantum chemical calculations at the B3P86/6-311+G(2df) and
6
7 MP2/6-311+G(2df) level of approximations that yield an energy difference of ca. 1.5
8
9 and 0.9 kcal/mol, respectively.²² CF_3SNO is the only known primary thionitrite with a
10
11 marked preference for the *anti* form.
12

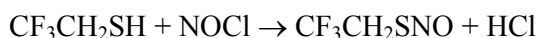
13
14
15 Prompted by these finding, we became interested in the conformational behavior
16
17 of the ethyl derivatives. In particular, we want to establish if the presence of fluorine
18
19 atoms asserts the conformational behavior through the so called "fluorine effect".³⁵
20
21 Since only few reports on the preparation³⁶ and fundamental properties³⁷ of
22
23 CH_3CH_2SNO exist in literature, in the present work ethyl- and 2,2,2-trifluoro ethyl
24
25 thionitrites, (CX_3CH_2SNO , $X = H$ and F) have been synthesized and their gas phase
26
27 infrared spectra fully analyzed accompanied by quantum-chemical calculations. It
28
29 should be remarked that CF_3CH_2SNO is a novel thionitrite derivative, for which the
30
31 preparation, proper isolation and characterization is provided within this contribution.
32
33
34
35
36
37

38 **2-Experimental Section**

39
40
41 The compounds were manipulated in a glass vacuum system equipped with
42
43 PTFE stems (Young valves) and greased joints if it is necessary. All experiments were
44
45 performed avoiding the presence of light. $NOCl$ was prepared from $NaCl$ and $NOHSO_4$
46
47 (Aldrich) following the reported method.³⁸ CH_3CH_2SNO was prepared from $NOCl$ and
48
49 CH_3CH_2SH (Aldrich, 95%).¹
50
51

52
53 Synthesis of CF_3CH_2SNO : This molecule was prepared following the general method
54
55 for the synthesis of $RSNO$ derivatives reported by Tasker and Jones.¹ In general it
56
57
58
59
60

1
2
3 consists in the reaction of nitrosyl chloride with mercaptans, according the following
4
5 equation:
6



8
9
10
11 In a typical preparation, slightly more than the stoichiometric amount of NOCl
12 was condensed onto 8 mmol of CF₃CH₂SH (Aldrich, 95%) maintained in vacuum in a
13 reaction ampoule cooled in liquid nitrogen. The reaction tube was warmed briefly to
14 melt the NOCl, re-cooled twice to -50 °C and maintained at that low temperature until a
15 bright red liquid was obtained. The tube was warmed to ca. -20°C and the mixture
16 purified by trap to trap distillation through traps held at -60, -90 and -196 °C. Pure
17 CF₃CH₂SNO (ca. 7 mmol, 87 %) was obtained as a red-brown liquid in the -60 °C trap.
18 HCl and minor quantities of NO were observed in the U-trap held at -196 °C.
19
20
21
22
23
24
25
26
27
28
29

30 Attempts to prepare CF₃CH₂SNO by the nitrite/thionitrite exchange method
31 were also conducted.³⁹ In this case equimolar quantities of *tert*-butyl nitrite (Across, 95
32 %) and CF₃CH₂SH were co-condensed in a Carius tube. The reaction occurs as
33 evidenced by the red coloration adopted by the reaction mixture at a temperature of -30
34 °C. However, the separation of the products mixture [presumably (CH₃)₃COH and
35 CF₃CH₂SNO] by using trap-to-trap distillation results much more difficult affecting the
36 yield of the desired compound.
37
38
39
40
41
42
43
44
45

46 The new compound is a red-brown liquid at room temperature, and
47 photosensitive in the presence of visible light. Signs of decomposition appear after 30
48 min of keeping a small sample at room temperature, as evidenced by the presence of
49 NO in the infrared spectrum of the vapor. The vapor pressure of CF₃CH₂SNO follows,
50 in the temperature range between 226 and 268 K, the equation $\log p = 12.0 - 3881/T$
51 (p/bar , T/K), and the boiling point can be extrapolated to be 51 °C.
52
53
54
55
56
57
58
59
60

1
2
3 The ^1H NMR spectrum only shows a quartet signal located at $\delta = 3.43$ ppm,
4
5 $^3J_{(\text{F,H})} = 9.8$ Hz, that corresponds to the CH_2 - group of the molecule. In the ^{19}F NMR
6
7 spectrum one triplet located at $\delta = -65.9$ ppm can be observed with the same $^3J_{(\text{F,H})}$
8
9 coupling. In addition, the ^{13}C NMR spectrum of the fluorinated title compound shows
10
11 two quartet signals at $\delta = 127.1$ ($^1J_{(\text{F,C})} = 277$ Hz) and 43.4 ($^2J_{(\text{F,C})} = 31$ Hz) ppm,
12
13 assigned to the carbon atoms of the CF_3 and CH_2 groups, respectively. These values are
14
15 in sound agreement with those reported for the related $(\text{CF}_3\text{CH}_2\text{S})_4\text{Sn}$ compound.⁴⁰
16
17 Additional evidence for the identity of $\text{CF}_3\text{CH}_2\text{SNO}$ can be gained from the analysis of
18
19 its gas IR spectrum, as discussed below.
20
21
22

23
24 Vibrational Spectroscopy: Gas-phase infrared spectra were recorded with a resolution of
25
26 1 cm^{-1} in the range $4000\text{--}400\text{ cm}^{-1}$ with a Bruker IFS 66v FTIR instrument.
27

28
29 Computational Methods: All quantum-chemical calculations were performed with the
30
31 Gaussian 03 program package.⁴¹ As suggested by Marazzi et al.²² MP2 and B3P86
32
33 methods⁴² and gradient techniques were used for the geometry optimizations and
34
35 vibrational properties, together with standard basis sets up to the Pople-type 6-
36
37 311+G(2df) basis set that includes diffuse and polarization functions, and Dunning's
38
39 correlation-consistent basis set of valence triple- ζ (cc-pVTZ). For comparison, other
40
41 classic hybrid functionals⁴³ (B3LYP⁴⁴ and B3PW91) were also applied. Optimization
42
43 geometry and frequencies were performed with Opt = VeryTight and Integral (Grid =
44
45 UltraFine) option, respectively. For the normal coordinate analysis, transformations of
46
47 the *ab initio* Cartesian harmonic force constants to the molecule-fixed internal
48
49 coordinates system were performed, as described by Hedberg and Mills and
50
51 implemented in the ASYM40 program.⁴⁵ This procedure evaluates the potential energy
52
53 distribution (PED) associated with each normal vibrational mode under the harmonic
54
55 assumption. The internal and symmetry coordinates used to perform the normal
56
57
58
59
60

1
2
3 coordinate analysis are defined in Figure S1 and Table S1, in the Supporting
4
5 Information.
6
7
8
9

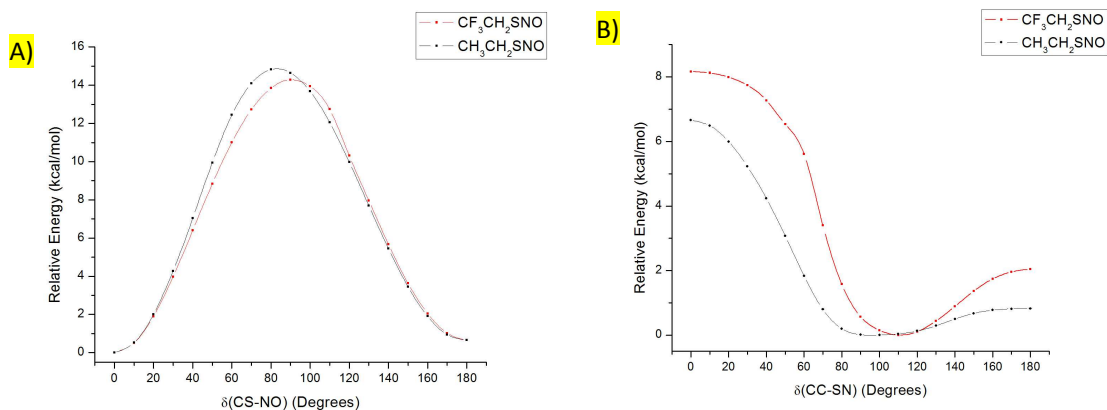
10 11 **3-Results and discussion**

12 13 14 *3.1-Conformational analysis*

15
16 The potential energy curves for the internal rotation around C–S and S–N bonds
17
18 were obtained by structure optimization at fixed dihedral angles from 0 to 180° in steps
19
20 of 10°, at the B3P86/6-311+G(2df) level of approximation, for both CH₃CH₂SNO and
21
22 CF₃CH₂SNO compounds. As shown in Figure 1 (left), the potential energy curves for
23
24 rotation around the S–N bond are similar, with two minima at 0 and 180°. In both cases,
25
26 the most stable form corresponds to the *syn* conformation (C–S single and N=O double
27
28 bonds in mutual synperiplanar orientation). The *anti* conformer is observed higher in
29
30 energy by around 0.7 kcal/mol, with C–S single and N=O double bonds in
31
32 antiperiplanar conformation. The curves are nearly symmetrical with respect to a local
33
34 maximum at $\delta(\text{CS-NO}) = 90^\circ$, corresponding to a torsional transition state with a
35
36 computed energy barrier to internal rotation of 15.2 kcal/mol (CH₃CH₂SNO) and 14.1
37
38 kcal/mol (CF₃CH₂SNO). The computed [B3P86/6-311+G(2df)] geometries for the
39
40 transition states of CF₃CH₂SNO and CH₃CH₂SNO give similar $\delta(\text{CS-NO})$ values (82.5
41
42 and 82.9°, respectively). The S–N bond is elongated with respect to the minimum
43
44 geometry (see Section 3.2), reaching values of 2.007 and 1.942 Å, while the N=O bond
45
46 is reinforced, with $r(\text{N=O})$ bond lengths of 1.145 and 1.158 Å for the transition states of
47
48 CF₃CH₂SNO and CH₃CH₂SNO, respectively. Thus, strong electronic reorganizations
49
50 occur upon S–N bond rotation, doubtless affecting the high of the rotational barrier.
51
52
53
54
55
56
57
58
59
60

1
2
3
4
5
6
7
8
9
10
11
12
13
14
15
16
17
18
19
20
21
22
23
24
25
26
27
28
29
30
31
32
33
34
35
36
37
38
39
40
41
42
43
44
45
46
47
48
49
50
51
52
53
54
55
56
57
58
59
60

Figure 1 (right) shows the potential energy curves calculated for the internal rotation around the C–S bond of $\text{CF}_3\text{CH}_2\text{SNO}$ and $\text{CH}_3\text{CH}_2\text{SNO}$, corresponding to the formal rotation of the 2,2,2-trifluoroethyl and ethyl groups with respect to the –SNO group, respectively. For both compounds, the global minimum corresponds to a structure with gauche conformation, with $\delta(\text{CC–SN}) \approx 110^\circ$ for $\text{CF}_3\text{CH}_2\text{SNO}$, while the corresponding minimum for the ethyl derivative lies in a flat portion of the potential energy curve. It is important to notice that both the *syn* and *anti* conformations around the C–S bond [$\delta(\text{CC–SN}) = 180^\circ$] are located in a local maxima in the potential energy curve. Further harmonic frequency calculations allowed to assign the anti form as a rotational transition state connecting two energetically equivalent forms of the *gauche* rotamer (\pm -*gauche*). The computed barriers are 1.0 and 2.1 kcal/mol, higher for the 2,2,2-trifluoroethyl derivative, suggesting the influence at least of steric factors for the bulky CF_3CH_2 - moiety.



1
2
3 **Figure 1.** Calculated [B3P86/6-311+G(2df)] potential energy function for internal
4 rotation around S–N (A) and C–S (B) single bonds in CF₃CH₂SNO (red line) and
5 CH₃CH₂SNO (black line).
6
7
8
9

10
11
12 Full geometry optimizations and frequency calculations for each of the most
13 stable structures have been performed by using DFT and MP2(full) methods with
14 relative large basis sets [6-311+G(2df) and cc-pVTZ]. Following Marazzi et al.²² three
15 hybrid functional (B3P86, B3LYP and B3PW91) have been applied. The optimized
16 structure of the *syn* and *anti* conformers of CF₃CH₂SNO and CH₃CH₂SNO are shown in
17 Figure 2. The results obtained at all tested level of approximations are in accordance
18 with the fact that the *syn* form is more stable than the *anti* one. The computed energy
19 difference (corrected by zero point energy) and Gibbs free energy differences (in
20 kcal/mol) between the *anti* and *syn* forms are listed in Table 1. It can be observed that
21 the cc-pVTZ polarized Dunning's type basis set systematically gives slightly higher
22 differences in energy values than the Pople-type basis set 6-311+G(2df) with
23 polarization and diffuse functions. Difference energy values (ΔE^0) computed with the
24 same method of approximations with less extended basis sets are given in Table S2
25 (Supporting Information). For both compounds, the ΔE^0 computed with the 6-31G(d) is
26 much larger than that obtained with more extended basis sets.
27
28
29
30
31
32
33
34
35
36
37
38
39
40
41
42
43
44

45 As was previously observed for other thioinitrites,²² the explicit inclusion of
46 electron correlation in the MP2 method computes higher energy differences than those
47 obtained by using DFT methods.
48
49
50

51
52 Accordingly to the Boltzmann distribution and by taking into consideration the
53 calculated ΔG^0 values at the MP2(full)/cc-pVTZ level of approximation, a relative
54
55
56
57
58
59
60

abundance of roughly 21 and 26 % of the less stable *anti* form is expected to be present at room temperature in the vapor of $\text{CF}_3\text{CH}_2\text{SNO}$ and $\text{CH}_3\text{CH}_2\text{SNO}$, respectively.

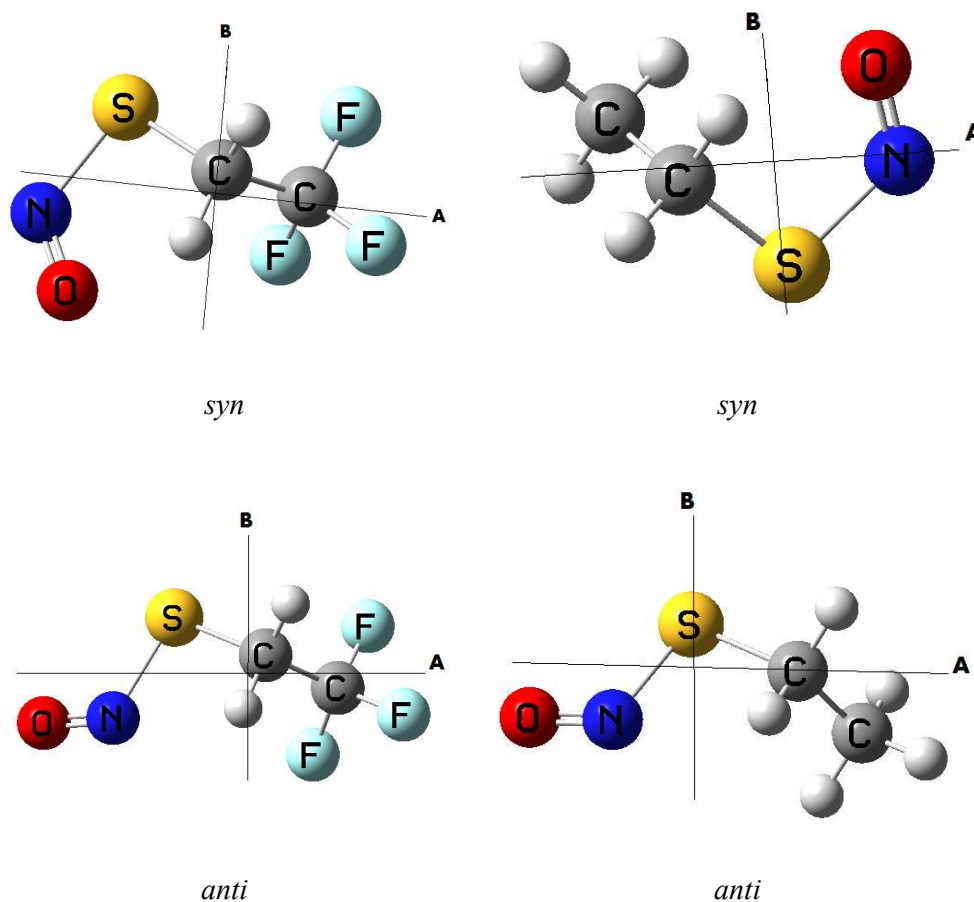


Figure 2. Molecular models for the two main conformers of $\text{CF}_3\text{CH}_2\text{SNO}$ (left) and $\text{CH}_3\text{CH}_2\text{SNO}$ (right). Principal axes of inertia are displayed (the *C*-axis is perpendicular to the plane formed by the *A*- and *B*-axes).

Table 1. Calculated relative energy (corrected by zero-point energy) and Gibbs free energy differences (in kcal/mol) for $\text{CX}_3\text{CH}_2\text{SNO}$ ($\text{X} = \text{F}$ and H) and concentration of the most stable *syn* forms.

Level of approximation		CF ₃ CH ₂ SNO			CH ₃ CH ₂ SNO		
		ΔE°	ΔG°	%	ΔE°	ΔG°	%
B3P86	6-311+G(2df)	0.65	0.52	71	0.68	0.82	80
	cc-pVTZ	0.75	0.65	75	0.79	0.92	83
B3LYP	6-311+G(2df)	0.37	0.25	60	0.42	0.44	68
	cc-pVTZ	0.52	0.43	68	0.58	0.66	75
B3PW91	6-311+G(2df)	0.46	0.34	64	0.51	0.64	75
	cc-pVTZ	0.56	0.46	69	0.61	0.71	77
MP2(full)	6-311+G(2df)	0.86	0.60	74	1.04	0.39	66
	cc-pVTZ	1.02	0.78	79	1.24	0.63	74

3.2- Molecular structure

It was reported⁴⁶ that different quantum chemical methods with an appropriate large basis set generally give optimized structures of RSNOs, in close agreement with each other. The B3P86/6-311+G(2df) and MP2(full)/cc-pVTZ computed geometrical parameters for optimized molecular structures for *syn* and *anti* conformers of CH₃CH₂SNO and CF₃CH₂SNO are given in Table 2. For completeness, the results obtained for the most stable *syn* conformer, computed at the same methods with the less extended 6-31G(d) and 6-311+G(d) basis sets are given in Table S3 in the Supporting Information.

Table 2. Computed geometrical parameters (distances in Å, angles in deg) for *syn* and *anti* conformers of CX₃CH₂SNO (X = H and F) at different levels of approximation.

Parameter	CF ₃ CH ₂ SNO	CH ₃ CH ₂ SNO

	B3P86		MP2(full)		B3P86		MP2(full)	
	6-311+G(2df)		cc-pVTZ		6-311+G(2df)		cc-pVTZ	
	<i>syn</i>	<i>anti</i>	<i>syn</i>	<i>anti</i>	<i>syn</i>	<i>anti</i>	<i>syn</i>	<i>anti</i>
$r(\text{N}=\text{O})$	1.174	1.168	1.182	1.178	1.183	1.178	1.202	1.194
$r(\text{S}-\text{N})$	1.823	1.835	1.850	1.853	1.792	1.803	1.775	1.796
$r(\text{C}-\text{S})$	1.787	1.792	1.780	1.787	1.799	1.805	1.794	1.800
$r(\text{C}-\text{C})$	1.510	1.511	1.501	1.502	1.518	1.516	1.514	1.513
$\angle(\text{SNO})$	117.5	116.4	116.3	116.1	117.5	116.7	116.3	116.0
$\angle(\text{NSC})$	101.3	93.5	99.4	91.8	102.5	95.2	100.8	93.7
$\angle(\text{CCS})$	113.9	113.7	113.4	113.3	113.8	113.6	112.8	113.1
$\angle(\text{SCH})$	106.8	108.6	108.7	108.7	105.9	106.0	106.1	106.0
$\angle(\text{CCH})$	108.5	108.5	108.3	108.3	111.5	111.6	111.6	111.6
$\angle(\text{HCH})$	109.0	108.9	109.4	109.4	107.7	107.6	108.3	108.1
$\angle(\text{XCC})$	111.3	111.3	111.2	111.2	110.9	110.9	110.5	110.5
$\angle(\text{XCX})$	107.5	107.6	107.7	107.7	108.0	108.0	108.4	108.4
$\delta(\text{CS-NO})$	0.4	179.4	0.4	178.0	0.3	179.0	0.5	177.9
$\delta(\text{NS-CC})$	110.1	107.9	98.9	102.5	97.9	107.7	83.6	97.8
$\delta(\text{SC-CX})$	179.3	179.3	178.6	179.8	179.8	179.0	179.0	179.4

The computed [MP2(full)/cc-pVTZ] values for $r(\text{N}=\text{O})$ and $r(\text{S}-\text{N})$ bond length of the *syn* form of $\text{CH}_3\text{CH}_2\text{SNO}$, i.e. 1.202 and 1.775 Å, respectively, are in reasonable agreement with those previously reported (1.188 and 1.792 Å) at the QCISD/6-311G(df,p) level of approximation.⁴⁶ The N=O bond is longer for the *syn* conformers of both compounds here studied. On the other hand, and in agreement with previous

1
2
3 results²² for primary RSNO compounds, the S–N bond is longer in the *anti* than in *syn*
4
5 conformer. As suggested by Timerghazin et al.^{11,13} the repulsion of lone pairs of
6
7 electrons between sulfur and oxygen may be responsible for the longer N=O bonds
8
9 found in *anti* RSNO compounds.
10

11
12 Interestingly, the larger difference in the geometrical parameters between both
13 conformers is evidenced by the CSN bond angle for both CH₃CH₂SNO and
14 CF₃CH₂SNO compounds. In effect, the MP2(full)-cc-pVTZ computed values for
15 $\angle(\text{CSN})$ are 91.8 and 93.7 degrees for the *anti* rotamer of CH₃CH₂SNO and
16 CF₃CH₂SNO, respectively, which are around 8° smaller than that in the *syn* form. This
17 tendency can also be rationalized by steric effects acting in the *syn* form, mainly due to
18 the repulsion of both lone pairs of electrons formally located at the sulfur and oxygen
19 atoms.
20
21
22
23
24
25
26
27
28
29
30

31 When the computed geometrical parameters are compared between CF₃CH₂SNO
32 and CH₃CH₂SNO, important differences are found, especially in the thionitrite group.
33 Both methods reproduce the same trend, and the MP2(full)/cc-pVTZ will be further
34 considered. In effect, the N=O bond is shorter in the fluorinated compound by 0.02 Å,
35 while the S–N bond is longer by 0.075 Å. In agreement with recent results on RSNO
36 compounds,⁴⁶ the S–N bond in CX₃CH₂SNO (X = H and F) should be considered as a
37 single bond, without double bond character, as was early assumed.⁴⁷ Moreover, such a
38 weaker S–N bond for CF₃CH₂SNO may be a factor to explain the high instability
39 experimentally observed for this compound.
40
41
42
43
44
45
46
47
48
49
50

51 52 53 54 55 3.3-Vibrational analysis 56 57 58 59 60

1
2
3 Figures 3 and 4 show the FTIR spectra of gaseous CH₃CH₂SNO and
4
5 CF₃CH₂SNO, respectively. Frequency calculations at the MP2(full)/cc-pVTZ level of
6
7 approximation have been performed to assist the analyses of the experimental results. A
8
9 tentative assignment of the observed bands was carried out based on the calculated
10
11 displacement vectors for the fundamentals, as well on comparison with the spectra of
12
13 related molecules, particularly CX₃SNO (X = F³⁴ and H²⁶⁻²⁹). The previous vibrational
14
15 analysis reported for the CH₃CH₂SNO species has been especially considered in the
16
17 light of the new available data.³⁷ Furthermore, the PED associated with each normal
18
19 vibrational mode has been calculated under the harmonic assumption. From PED
20
21 analysis, it becomes clear that, as expected, many vibrations have a high degree of
22
23 mixture. Therefore, tentative assignments for characteristic and intense spectral features
24
25 in the vibrational spectra of the molecules are discussed. Tables 3 and 4 list the
26
27 vibrational results for CH₃CH₂SNO and CF₃CH₂SNO, respectively.
28
29
30

31
32 It is well-known that the detailed analysis of band contours in infrared spectra
33
34 can provide valuable information regarding the gas-phase structure of rotamers.⁴⁸⁻⁵⁰ The
35
36 experimentally observed band contours for CF₃CH₂SNO and CH₃CH₂SNO are also
37
38 listed in Tables 3 and 4. Calculated rotational constants (cm⁻¹) and molecular
39
40 parameters, together with the estimated separation between P and R branches [$\Delta\nu(\text{PR})$
41
42 values, in cm⁻¹] – as obtained following the classical method of Seth-Paul⁵¹ – are
43
44 collected in Table 5. Both molecules can be classified as prolate asymmetric rotors. It
45
46 should be noted that since relative high ρ^* values ($\rho^* > 1$) are computed, the PQQR band
47
48 structure expected for B-type contours passes into a band structure with only two
49
50 maxima (PQ and QR) branches.
51
52

53
54
55
56 CH₃CH₂SNO
57
58
59
60

1
2
3 A tentative assignment for infrared spectrum of ethyl thionitrite, $\text{CH}_3\text{CH}_2\text{SNO}$,
4
5 was early reported by Philippe and Moore,³⁷ by assuming that alkyl thionitrite
6
7 molecules belong to the C_s point group of symmetry. However, with the help of
8
9 quantum-chemical calculations, it was clearly demonstrated that $\text{CH}_3\text{CH}_2\text{SNO}$ adopts
10
11 C_1 symmetry.⁴⁶ The calculated [MP2(full)/cc-pVTZ] symmetry parameter ($\kappa = -0.42$)
12
13 for *syn* $\text{CH}_3\text{CH}_2\text{SNO}$ with C_1 symmetry indicates that the molecule can also be
14
15 classified as prolate asymmetrical top. When compared with the 2,2,2-trifluoro
16
17 derivative, higher separations between P- and R- branches are calculated, in agreement
18
19 with the lower mass of the hydrogen with respect to the fluorine atoms. The $\Delta\nu(\text{PR})$
20
21 expected for the most stable *syn* conformer amounts 16.4, 12.6 and 24.6 cm^{-1} of the A,
22
23 B and C type-bands, respectively.
24
25
26

27 The spectrum of $\text{CH}_3\text{CH}_2\text{SNO}$ clearly shows bands associated with the CH_3
28
29 antisymmetric modes of vibration at 2988 and 2981 cm^{-1} and the totally symmetric
30
31 vibration of the CH_3 group at 2888 cm^{-1} . The 2945 cm^{-1} band with a definite PQR
32
33 structure can be assigned to C–H antisymmetric stretching mode of the $-\text{CH}_2-$ group.
34
35

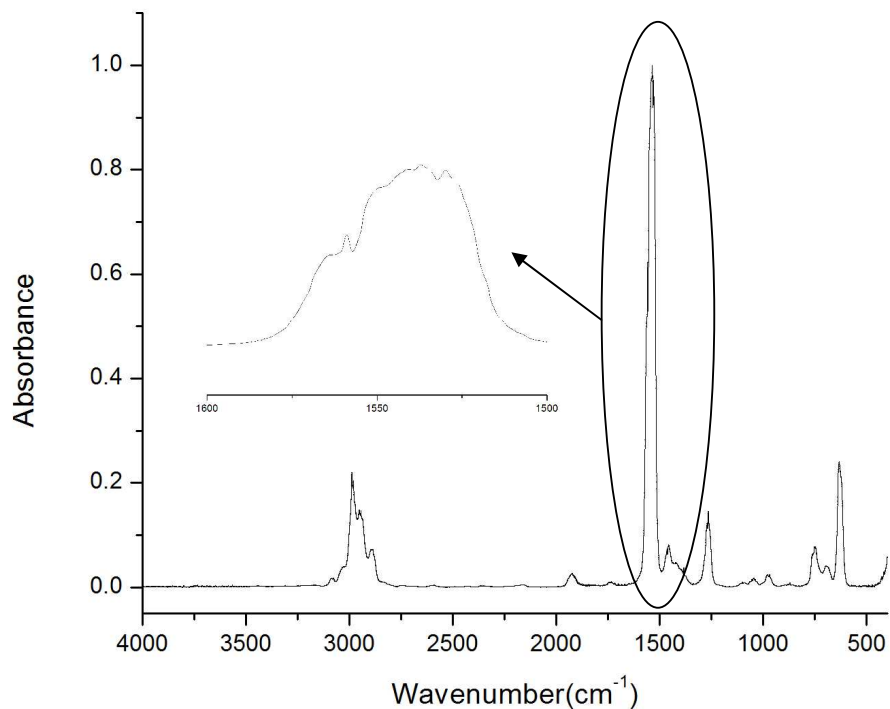
36 The stretching mode $\nu(\text{N}=\text{O})$ and its first overtone can be used to solve one of
37
38 the fundamental questions in the present study testing the conformational equilibrium of
39
40 this and the partially fluorinated species. This normal mode of vibration can be assigned
41
42 to a strong and broad band with an approximated B contour and maxima at 1538 and
43
44 1530 cm^{-1} , in perfect agreement with the previously reported value of 1534 cm^{-1} .³⁷ Its
45
46 B-type envelope can be originated from the quasi parallelism of this oscillator in
47
48 relation with the B principal moment of inertia (Figure 2). It is interesting to note that,
49
50 superimposed to this band at higher energies and centered at 1559 cm^{-1} an A-type band
51
52 is observed in the gas infrared spectrum (see Figure 3, inset). It is reasonable to assume
53
54 that this absorption corresponds to the N=O stretching vibration of the *anti* form, in
55
56
57
58
59
60

1
2
3 agreement with the relative orientation of this oscillator with respect to the principal
4 moments of inertia depicted in the Figure 2. The branch separations for these A and B
5 bands also agree quite well with the calculated results listed in Table 5. The assignment
6 related to the N=O stretching vibrations to the two rotamers is confirmed by the
7 evaluation of their N=O overtones. Centered in 3083 and 3034 cm^{-1} two weak bands
8 with B and A contours, respectively, can be observed in the FTIR spectrum of the
9 gaseous sample. These bands can be straightforward assigned to the first N=O
10 stretching vibration overtones belonging to both the *anti* and the *syn* conformation,
11 respectively, taken into account their contours, relative intensities and the duplication of
12 the wavenumbers difference with relation to their two fundamental modes (49 cm^{-1} in
13 case of the first overtones and 25 cm^{-1} for the N=O fundamental mode of vibration).
14 The MP2(full)/cc-pVTZ computed frequency values for the $\nu(\text{N=O})$ fundamentals are
15 too low (1524 and 1492 cm^{-1} for the *anti* and *syn* conformers, respectively).
16
17
18
19
20
21
22
23
24
25
26
27
28
29
30
31

32 In agreement with the previously reported vibrational assignment,³⁷ the bands at
33 1464, 1457 and 1384 cm^{-1} are tentatively associated with the deformation motions of
34 the CH_3 and CH_2 groups.
35
36
37

38 As recognized by Philippe and Moore,³⁷ the assignment of vibrations such as the
39 C–S and N–S stretching and C–H and S–N=O deformation modes is not
40 straightforward. Therefore and based on the results derived from both, the band contour
41 analysis and quantum chemical calculations, a tentative assignment is presented in
42 Table 3. The weak absorptions at 1045 cm^{-1} and the B-type band centered at 974 cm^{-1}
43 could originate from the $\nu(\text{C–C})$ and $\rho_{\text{ac}}(\text{CH}_3)$ fundamental modes of vibration. More
44 important, on the basis of the potential energy distribution analysis, the band centered at
45 693 cm^{-1} is now assigned to the $\nu(\text{C–S})$ stretching vibration. The AB-type band
46 observed with medium intensity centered at 629 cm^{-1} is generated by the $\delta(\text{SNO})$
47
48
49
50
51
52
53
54
55
56
57
58
59
60

1
2
3 motion, in good agreement with the computed value (648 cm^{-1}). Our MP2(full)/cc-
4
5 pVTZ results suggest that the $\nu(\text{S-N})$ stretching mode contributes to a vibration
6
7 appearing near 400 cm^{-1} (the computed value for the *syn* form is 398 cm^{-1}). As
8
9 observed in Figure 3, an incomplete band rises below the limit of our spectrophotometer
10
11
12
13
14
15
16
17
18
19
20
21
22
23
24
25
26
27
28
29
30
31
32
33
34
35
36
37
38
39



40
41
42
43
44
45
46
47
48
49
50
51
52
53
54
55
56
57
58
59
60
Figure 3. Gas phase FTIR of $\text{CH}_3\text{CH}_2\text{SNO}$ at 11 mbar (glass cell, 10 cm optical path length, KBr windows, 2 mm thick). The inset shows the enlargement of the $\nu(\text{N=O})$ absorption band.

Table 3: Observed and Calculated [MP2(full)/cc-pVTZ] Vibrational Data (cm⁻¹) for CH₃CH₂SNO

IR (gas) ^a	Band contour. ($\Delta\nu(\text{PR})$)	MP2(full)/cc-pVTZ ^b		Tentative assignment
		<i>syn</i>	<i>anti</i>	
3089 QR (vw) 3078 QP (vw)	B (11)			2*v(N=O) anti
3041 R 3034 Q (vw) 3029 P	A (12)			2*v(N=O) syn
2988 (vw)		3187(4)	3183 (5)	$\nu_{\text{as}}\text{CH}_3(90)+\nu_{\text{as}}(\text{CH}_2)(10)$
2981 (vw)		3172(6)	3168 (7)	$\nu_{\text{as}}\text{CH}_3(100)$
2953 R 2945 Q(vw) 2938 P	A (15)	3155(0.3)	3154 (0.4)	$\nu_{\text{as}}(\text{CH}_2)(80)+\nu_{\text{s}}(\text{CH}_3)(10)+\nu_{\text{s}}(\text{CH}_2)(10)$
		3100(4)	3107 (4)	$\nu_{\text{s}}(\text{CH}_2)(70)+\nu_{\text{s}}(\text{CH}_3)(20)+\nu_{\text{as}}(\text{CH}_2)(10)$
2888 (vw)		3099(7)	3095 (8)	$\nu_{\text{s}}(\text{CH}_3)(80)+\nu_{\text{s}}(\text{CH}_2)(20)$
2167(vw)				$\nu(\text{N=O})+\delta(\text{SNO})$
1923(vw)				$\nu(\text{N=O})+\nu(\text{S-N})$
1564 R 1559 Q (vs) 1550 P	A (14)		1524 (100)	$\nu(\text{N=O})(80)+\delta_{\text{as}}(\text{CH}_2)(20)$ (anti)
1538 QR (s) 1530 QP (s)	B (8)	1492(100)		$\nu(\text{N=O})(65)+\rho(\text{CH}_2)(20)$ (syn)
1464 (vw)		1457(27)	1478 (2)	$\rho(\text{CH}_2)(80)+\nu(\text{N=O})(20)$
		1525(2)	1522 (29)	$\delta_{\text{as}}(\text{CH}_3)(100)$

1457 (vw)		1521(0.5)	1520 (37)	$\delta_{\text{as}}(\text{CH}_3)(100)$
		1421(4)	1423 (2)	$\delta_{\text{s}}(\text{CH}_3)(100)$
1384 (vw)		1307(10)	1315 (7)	$\rho_{\text{as}}(\text{CH}_2)(85)+\rho_{\text{s}}(\text{CH}_2)(15)$
1272 R 1265 Q (vw) 1259 P	AC (23)	1294(1)	1299 (3)	$\rho_{\text{s}}(\text{CH}_2)(80)+\rho_{\text{as}}(\text{CH}_3)(20)$
1045 (vw)		1096(1)	1102 (0.1)	$\nu(\text{C-C})(60)+\rho_{\text{as}}(\text{CH}_3)(40)$
		1062(1)	1067 (3)	$\rho_{\text{as}}(\text{CH}_3)(50)+\rho_{\text{s}}(\text{CH}_2)(35)+\rho(\text{CH}_2)(15)$
981 (vw) QR 971 (vw) QP	B (10)	1007(2)	1011 (3)	$\rho_{\text{as}}(\text{CH}_3)(45)+\nu(\text{C-C})(45)+\rho_{\text{as}}(\text{CH}_2)(10)$
752 (vw)		768(21)	761 (5)	$\rho(\text{CH}_2)(40)+\delta(\text{SNO})(30)+\rho_{\text{as}}(\text{CH}_3)(30)$
693 (vw)		713(1)	721 (5)	$\nu(\text{C-S})(80)+\rho(\text{CH}_2)(20)$
635 (w) R 623 (w) P	AB (12)	648(33)	658 (66)	$\delta(\text{SNO})(60)+\rho(\text{CH}_2)(25)+\nu(\text{S-N})(15)+\nu(\text{C-S})(10)$
		398(68)	394 (41)	$\nu(\text{S-N})(100)$
		371(4)	327 (7)	$\delta(\text{CCS})(55)+\tau(\text{CS-NO})(45)$
		305(3)	292 (6)	$\tau(\text{HC-CS})(55)+\delta(\text{CSN})(45)$
		248(0.2)	211 (0.1)	$\tau(\text{CS-NO})(65)+\delta(\text{CCS})(35)$
		210(3)	194 (8)	$\tau(\text{CS-NO})(50)+\delta(\text{CSN})(50)$
		91(0.4)	38 (0.1)	$\tau(\text{CC-SN})(100)$

^a Band Intensity: vs = very strong, s = strong, m = medium, w = weak, vw = very weak. ^b In parentheses relative band strengths for the two most stable forms, IR intensities (100% = 204 km/mol for *syn-gauche* form and 100% = 220 km/mol for the *anti* form). ^c Unless indicated, band assignment and PED values correspond to the most stable conformer, only contribution larger than 10% are given.

CF₃CH₂SNO

The calculated [MP2(full)/cc-pVTZ] symmetry parameter ($\kappa = -0.84$) for *syn* CF₃CH₂SNO indicates that the molecule can be classified as prolate asymmetrical top. The expected separation between P- and R- branches are 9.8, 7.8 y 14.6 cm⁻¹ of the A, B and C type-bands, respectively. Slightly minor separations are expected for the *anti* conformer, as also listed in Table 5. However, rather distinctive the A, B and C band contours can be originated from both *syn* and *anti* conformers, depending on the relative orientation of the transition dipole moments with respect to the *A*, *B*, and *C* principal axis of inertia.

As earlier mentioned the gas phase IR spectrum of RSNOs is characterized by a strong absorption appearing in the 1700–1500 cm⁻¹ range, that correspond to the $\nu(\text{N}=\text{O})$ stretching mode.³⁷ This mode is quite sensitive to the nature of the R substituent. For CH₃SNO the corresponding values are 1548 and 1527 cm⁻¹ for the *anti* and *syn* forms, respectively, as determined from matrix isolation experiments.³⁰ For the related CF₃SNO species in its more stable anti conformation, this mode is observed at 1700 and 1660 cm⁻¹ in the infrared spectra of the solid and vapor, respectively.³⁴

In line with this tendency, the N=O stretching vibrations of the *anti*- and *syn*-CF₃CH₂SNO are observed at higher wavenumbers than that of the analogous rotamers of CH₃CH₂SNO. Thus, a well-defined absorption with PQR structure at 1605 cm⁻¹ is assigned to the N=O stretching vibration of the anti form taken into account the envelope and the comparison with the computed results (Table 4). At lower wavenumbers another absorption with a B-type contour centered at 1580 cm⁻¹ can be assigned to the N=O stretching vibration of the more abundant *syn* rotamer. As in case of the parent methylated molecule the evaluation of the N=O overtone region is

1
2
3 indicative to establish the conformational behavior of the molecule. As in case of the
4
5 former analyzed species and centered at 3173 (B-contour) and 3127 cm^{-1} (A-contour)
6
7 two bands can be assigned to the first N=O overtone of both the *anti* and *syn*
8
9 conformers, respectively, in view of their envelopes, band separation, relative intensity
10
11 and the difference between them as compared with N=O normal mode of vibration (46
12
13 and 25 cm^{-1} , respectively).
14
15

16 The $\nu(\text{C-F})$ stretching vibrations for CF_3SNO were assigned to three strong
17
18 absorptions observed in the infrared spectrum at 1140 (A''), 1100 (A') and the totally
19
20 symmetric at 1083 cm^{-1} .³⁴ In the $\text{CF}_3\text{CH}_2\text{SNO}$ spectrum, the strong absorptions
21
22 centered at 1148 cm^{-1} (with PQR structure) and the B-band at 1093 cm^{-1} are assigned to
23
24 these C-F antisymmetric stretching modes.
25
26

27 It is rather difficult to assign with confidence the $\nu(\text{C-S})$ and $\nu(\text{S-N})$ stretching
28
29 vibrations in $\text{CF}_3\text{CH}_2\text{SNO}$, since both vibrational modes are sensitive to substitution at
30
31 the sulfur. For example, extreme differences are reported for the C-S stretching
32
33 vibration where the $\nu(\text{C-S})$ normal mode appears at 731 cm^{-1} in CH_3SNO and decreases
34
35 upon fluorine substitution to 442 cm^{-1} in CF_3SNO .³⁴ On the other hand, the $\nu(\text{S-N})$
36
37 mode is found at 759 cm^{-1} in CF_3SNO ,³⁴ a higher value than for CH_3SNO , at 649 cm^{-1} .
38
39 In qualitative agreement with these features, a band of medium intensity with an A-
40
41 contour centered at 781 cm^{-1} is observed in the infrared spectrum of $\text{CF}_3\text{CH}_2\text{SNO}$,
42
43 which is tentatively assigned to the $\nu(\text{C-S})$ stretching, while the $\nu(\text{S-N})$ is computed at
44
45 295 cm^{-1} , below the cut-off of the KBr windows used in the measurements and the limit
46
47 of our spectrometer.
48
49
50
51
52
53
54
55
56
57
58
59
60

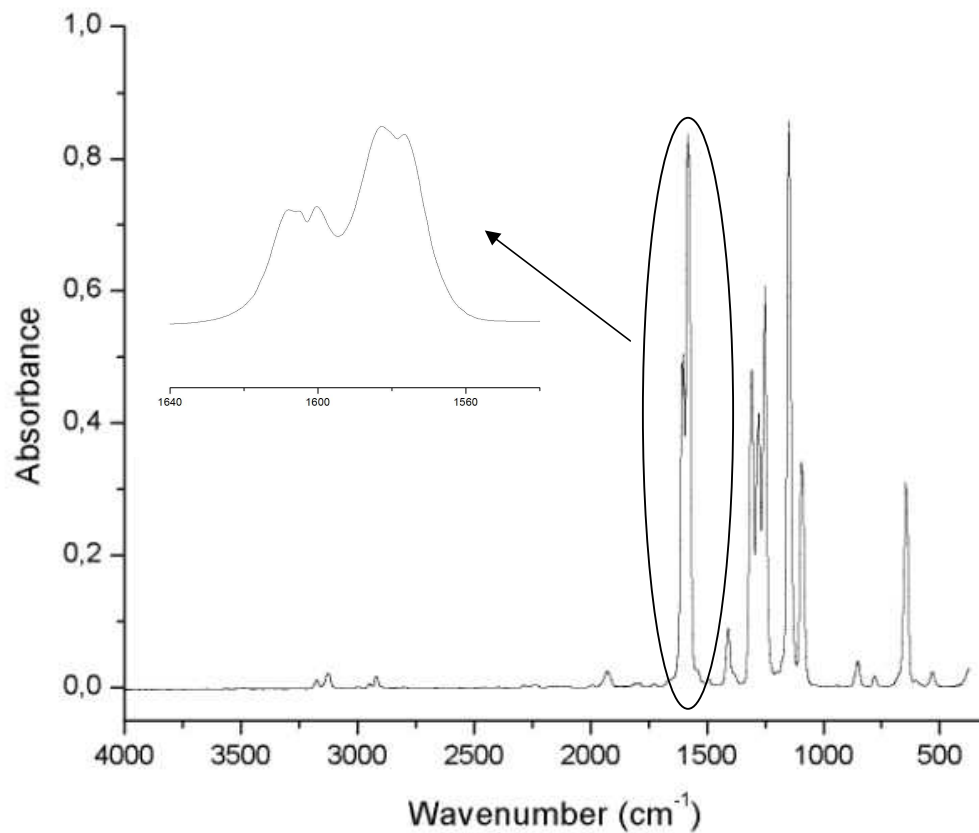


Figure 4. Gas phase FTIR at 10.0 mbar of $\text{CF}_3\text{CH}_2\text{SNO}$ (glass cell, 10 cm optical path length, KBr windows, 2 mm thick). The inset shows the enlargement of the $\nu(\text{N}=\text{O})$ absorption bands.

Table 4. Observed and Calculated [MP2(full)/cc-pVTZ] Vibrational Data (cm⁻¹) for CF₃CH₂SNO

IR (gas) ^a	Band contour. ($\Delta\nu(\text{PR})$)	MP2(full)/cc-pVTZ ^b		Tentative assignment (PED)
		<i>syn</i>	<i>anti</i>	
3176 QR (vw) 3169 QP (vw)	B (7)			2*v(N=O) anti
3132 R 3127 Q (vw) 3123 P	A(9)			2*v(N=O) syn
3000 QR (vw) 2993 QP (vw)	B (7)	3187 (0.7)	3188 (0.2)	v _{as} (CH ₂)(70) + v _s (CH ₂)(30)
2951 R 2947 Q (vw) 2942 P	A (9)	3079 (3)	3115 (2)	v _s (CH ₂)(70) + v _{as} (CH ₂)(30)
2921 (vw)				?

2285 (vw)				$2^* \delta_s(\text{CH}_2)$
2234 (vw)				$\delta_{\text{as}}(\text{CH}_2) + \delta_{\text{as}}(\text{CH}_2)$
1930 (vw)				$\nu(\text{N}=\text{O}) + \delta(\text{SNO})$
1608 R 1605 Q (s) 1600 P	A (8)		1586 (100)	$\nu(\text{N}=\text{O}) (95) (\text{anti})$
1583 QR (vs) 1577 QP (vs)	B (6)	1572 (100)		$\nu(\text{N}=\text{O}) (100) (\text{syn})$
1408 (vw)		1452 (12)	1461 (6)	$\delta(\text{CH}_2)(80) + \nu(\text{C}-\text{C})(10) + \delta_{\text{as}}(\text{CH}_2)(10)$
1312 R 1308 Q (s) 1304 P	A (8)	1358 (46)	1367 (32)	$\nu(\text{C}-\text{C})(40) + \delta_{\text{as}}(\text{CH}_2)(25) + \nu_s(\text{CF}_3)(20) + \delta_s(\text{CF}_3)(15)$
1283 QR (s) 1277 PQ (s)	B (6)	1325 (41)	1326 (30)	$\rho(\text{CH}_2)(45) + \nu_{\text{as}}(\text{CF}_3)(45) + \delta_{\text{as}}(\text{CF}_3) (10)$

1254 R				
1251 Q (s)	A (8)	1287 (38)	1291 (28)	$\delta_{\text{as}}(\text{CH}_2)(45) + \nu_{\text{as}}(\text{CF}_3)(35) + \delta_{\text{s}}(\text{CF}_3)(10) + \nu_{\text{s}}(\text{CF}_3)(10)$
1246 P				
1151 R				
1148 Q (vs)	A (7)	1184 (65)	1186 (52)	$\nu_{\text{as}}(\text{CF}_3)(65) + \delta_{\text{as}}(\text{CH}_2)(25) + \delta_{\text{as}}(\text{CF}_3)(10)$
1144 P				
1096 QR (m)	B (6)	1131 (32)	1132 (17)	$\nu_{\text{as}}(\text{CF}_3)(50) + \rho(\text{CH}_2)(50)$
1090 QP (m)				
855 QR (w)	B (5)	884 (2)	886 (4)	$\nu_{\text{s}}(\text{CF}_3)(50) + \nu(\text{C-C})(30) + \nu(\text{C-S})(20)$
850 QP (w)				
		867 (0.9)	879 (3)	$\rho(\text{CH}_2)(75) + \nu_{\text{as}}(\text{CF}_3)(15) + \delta(\text{CSN})(10)$
784 R				
781 Q (vw)	A (8)	813 (1)	816 (0.6)	$\nu(\text{C-S})(60) + \nu_{\text{s}}(\text{CF}_3)(15) + \delta(\text{CCS})(15) + \rho_{\text{s}}(\text{CF}_3)(10)$
776 P				

		673 (24)	665 (28)	$\delta(\text{S-NO})(90) + \nu(\text{S-N})(10)$
648 QR (m) 643 QP (m)	B (5)	659 (6)	657 (7)	$\delta_s(\text{CF}_3)(70) + \delta(\text{CCS})(10) + \nu(\text{CC})(10) + \nu_s(\text{CF}_3)(10)$
534 QR (vw) 529 QP (vw)	B (5)	546 (1)	545 (1.4)	$\delta_{\text{as}}(\text{CF}_3)(70) + \delta_s(\text{CF}_3)(10) + \delta_{\text{as}}(\text{CF}_3)(10) + \nu(\text{C-S})(10)$
		541 (2)	544 (0.2)	$\delta_{\text{as}}(\text{CF}_3)(90) + \rho(\text{CH}_2)(10)$
		390 (1)	395 (7)	$\rho_{\text{as}}(\text{CF}_3)(45) + \rho(\text{CH}_2)(15) + \rho_s(\text{CF}_3)(15) + \delta(\text{CSN})(15) + \delta_{\text{as}}(\text{CF}_3)(10)$
		359 (1)	362 (0.7)	$\rho_{\text{as}}(\text{CF}_3)(35) + \rho_s(\text{CF}_3)(35) + \delta_{\text{as}}(\text{CF}_3)(15) + \nu(\text{C-S})(15)$
		294 (38)	293 (23)	$\nu(\text{S-N})(70) + \nu(\text{N=O})(15) + \tau(\text{CSNO})(15)$
		269 (20)	223 (0.2)	$\nu(\text{S-N})(50) + \tau(\text{CSNO})(40) + \nu(\text{N=O})(10)$
		235 (4)	208 (8)	$\delta(\text{CSN})(75) + \rho_{\text{as}}(\text{CF}_3)(15) + \nu(\text{S-N})(10)$
		170 (0.5)	179 (1)	$\delta(\text{CCS})(65) + \rho_{\text{as}}(\text{CF}_3)(25) + \nu(\text{S-N})(10)$
		73 (<0.1)	71 (0.2)	$\tau(\text{CF}_3)(85) + \delta(\text{CSN})(15)$
		51 (0.2)	42 (0.1)	$\tau(\text{CCSN})$

^a Band Intensity: vs = very strong, s = strong, m = medium, w = weak, vw = very weak. ^b In parentheses relative band strengths for the two most stable forms, IR intensities (100% = 324 km/mol for *syn-gauche* form and 100 % = 445 km/mol for the *anti* form). ^c PED values correspond to the most stable conformer, only contribution larger than 10% are given.

Table 5. Rotational constants (cm^{-1}), asymmetry parameters and P-R branch separation (cm^{-1}) calculated at the MP2(full)/cc-pVTZ for $\text{CX}_3\text{CH}_2\text{SNO}$ (X= H and F)

		<i>A</i>	<i>B</i>	<i>C</i>	κ	ρ^*	β	$S(\beta)$	$\Delta\nu(\text{PR})^b$		
									<i>A</i> ()	<i>B</i> (\perp)	<i>C</i> (\perp)
CH₃CH₂SNO	<i>syn</i>	0.1968	0.1157	0.0825	-0.420	0.988	0.701	1.33	16.44	12.62	24.65
	<i>anti</i>	0.3244	0.0753	0.0677	-0.437	3.411	3.552	1.18	12.86	10.86	19.29
CF₃CH₂SNO	<i>syn</i>	0.1016	0.0395	0.0341	-0.840	1.708	1.572	1.265	9.8	7.8	14.8
	<i>anti</i>	0.1215	0.0317	0.0296	-0.953	2.897	2.829	1.206	8.5	7.1	12.8

^a Asymmetry parameters: $\kappa = (2B - A - C)/(A - C)$, $\rho^* = (A - C)/B$, $\beta + 1 = A/B$ (prolate top), $\log S(\beta) = 0.712/(\beta + 4)^{1.13}$. ^b P-R band separation are defined and calculated according to Seth-Paul.⁵¹

4-Conclusion

A proper method for the preparation and isolation of pure $\text{CF}_3\text{CH}_2\text{SNO}$ has been achieved. The conformational, structural and vibrational properties have determined on the basis of a detailed analysis of the infrared spectrum augmented with the band envelope evaluation. The overall evaluation of the experimental and theoretical results suggests the existence of a mixture of two conformers of $\text{CF}_3\text{CH}_2\text{SNO}$ at room temperature in the gas phase, the *syn* form (N=O double bond adopting a *syn* orientation with respect to the S-C single bond) being preferred over the *anti* one [MP2(full)/cc-pVTZ computed $\Delta E^0 \approx 1$ kcal/mol]. A similar conformational behavior was determined for the related $\text{CH}_3\text{CH}_2\text{SNO}$ species.

The $\nu(\text{N}=\text{O})$ stretching band is one of the most intense absorptions observed in the infrared spectra of RSNO compounds and –as demonstrated here– it is sensitive to the conformation around the S-N bond. Its first overtone can be subsequently detected adding information to resolve the conformational problem. In order to better determine the frequency values expected for the *syn* and *anti* conformers of the studied molecules, quantum-chemical calculations at different level of approximations have been further performed, the results being collected in Table 6. When MP2 and DFT methods are compared, strong variations can be found in the computed values, the DFT frequencies are found systematically at higher values (ca. 100 cm^{-1}) than those computed at the MP2 level. It should be stressed that such a systematic difference is expected since longer N=O bonds are computed with the MP2 method, as has been commented before (see Table 1). All levels of approximations applied here agree with the fact that for both $\text{CF}_3\text{CH}_2\text{SNO}$ and $\text{CH}_3\text{CH}_2\text{SNO}$ molecules, the computed $\nu(\text{N}=\text{O})$ stretching modes of the *anti* conformations occurs at higher frequencies than those of the *syn* forms. Again,

1
2
3 this is in line with longer bond lengths computed for the *syn* conformers. The DFT
4
5 methods yield mean $\Delta\nu(\text{N}=\text{O}) = \nu(\text{N}=\text{O})_{\text{anti}} - \nu(\text{N}=\text{O})_{\text{syn}}$ values of 35, 34 and 32 cm^{-1}
6
7 for $\text{CH}_3\text{CH}_2\text{SNO}$ and 36, 36 and 34 cm^{-1} for $\text{CF}_3\text{CH}_2\text{SNO}$ when the B3P86, B3PW91
8
9 and B3LYP functional are used, respectively. For $\text{CH}_3\text{CH}_2\text{SNO}$ a similar value of $\Delta\nu =$
10
11 34 cm^{-1} is found with the MP2 method, but a definite lower difference is obtained for
12
13 $\text{CF}_3\text{CH}_2\text{SNO}$ with these methods (11 cm^{-1}).
14
15
16
17
18

19 **Table 6.** Observed and Calculated $\nu(\text{N}=\text{O})$ (cm^{-1}) for $\text{CH}_3\text{CH}_2\text{SNO}$ and $\text{CF}_3\text{CH}_2\text{SNO}$
20

		$\text{CH}_3\text{CH}_2\text{SNO}$			$\text{CF}_3\text{CH}_2\text{SNO}$		
		<i>syn</i>	<i>anti</i>	$\Delta\nu(\text{cm}^{-1})$	<i>syn</i>	<i>anti</i>	$\Delta\nu(\text{cm}^{-1})$
B3P86	6-311+G(2df)	1640	1673	33	1683	1717	34
	cc-pVTZ	1659	1696	37	1698	1736	39
B3PW91	6-311+G(2df)	1643	1674	31	1685	1719	34
	cc-pVTZ	1662	1697	35	1700	1738	38
B3LYP	6-311+G(2df)	1620	1652	32	1668	1700	32
	cc-pVTZ	1659	1676	17	1685	1721	36
MP2(full)	6-311+G(2df)	1443	1480	37	1536	1544	8
	cc-pVTZ	1492	1524	32	1572	1586	14
Experimental		1537	1559	22	1580	1605	25

48 5-Acknowledgments

49
50
51 The authors are grateful to Deutsche Forschungsgemeinschaft for support
52
53 through an international project. The Argentinean authors thank the Consejo Nacional
54
55 de Investigaciones Científicas y Técnicas (CONICET), the Agencia Nacional de
56
57
58
59
60

Promoción Científica y Tecnológica and the Facultad de Ciencias Exactas, Universidad Nacional de La Plata for financial support.

6- Supplementary data. The internal and symmetry coordinates used to perform the normal coordinate analysis are defined in Figure S1 and Table S1, respectively. Tables S2 and S3 give thermodynamic and geometrical data computed with 6-31G(d) and 6-311+G(d) basis sets. This material is available free of charge via the Internet at <http://pubs.acs.org>.

7- References

- (1) Tasker, H. S.; Jones, H. O. Action of Mercaptans on Acid Chlorides II. Acid Chlorides of Phosphorus, Sulphur and Nitrogen. *J. Chem. Soc.* **1909**, *95*, 1910-1918.
- (2) Petit, C.; Hoffmann, P.; Souchard, J.-P.; Labidalle, S. Synthesis and Characterization of New Aromatic Thionitrites. *Phosphorus, Sulfur Silicon Rel. Elem.* **1997**, *129*, 59-67.
- (3) Zolfigol, M. A. Silica Sulfuric Acid/NaNO₂ as a Novel Heterogeneous System for Production of Thionitrites and Disulfides under Mild Conditions. *Tetrahedron* **2001**, *57*, 9509-9511.
- (4) Soulère, L.; Sturm, J.-C.; Núñez-Vergara, L. J.; Hoffmann, P.; Périé, J. Synthesis, Electrochemical, and Spectroscopic Studies of Novel S-nitrosothiols. *Tetrahedron* **2001**, *57*, 7173-7180.
- (5) Williams, D. L. H. The Chemistry of S-Nitrosothiols. *Acc. Chem. Res.* **1999**, *32*, 869-876.

1
2
3 (6) Stamler, J. S.; Toone, E. J. The Decomposition of Thionitrites. *Curr.*
4
5 *Opinion Chem. Biol.* **2002**, *6*, 779-785.
6

7 (7) Bartberger, M. D.; Mannion, J. D.; Powell, S. C.; Stamler, J. S.; Houk, K.
8
9 N.; Toone, E. J. S-N Dissociation Energies of S-Nitrosothiols: On the Origins of
10
11 Nitrosothiol Decomposition Rates. *J. Am. Chem. Soc.* **2001**, *123*, 8868-8869.
12
13

14 (8) Stamler, J. S.; Jaraki, O.; Osborne, J.; Simon, D. I.; Keaney, J.; Vita, J.;
15
16 Singel, D.; Valeri, C. R.; Loscalzo, J. Nitric Oxide Circulates in Mammalian Plasma
17
18 Primarily as an S-nitroso Adduct of Serum Albumin. *PNAS* **1992**, *89*, 7674-7677.
19

20 (9) Zhang, S.; Çelebi-Ölçüm, N.; Melzer, M. M.; Houk, K. N.; Warren, T. H.
21
22 Copper(I) Nitrosyls from Reaction of Copper(II) Thiolates with S-Nitrosothiols:
23
24 Mechanism of NO Release from RSNOs at Cu. *J. Am. Chem. Soc.* **2013**, *135*, 16746-
25
26 16749.
27
28

29 (10) Schmaunz, A.; Kensy, U.; Slenczka, A.; Dick, B. Photolysis of tert-
30
31 Butylthionitrite via Excitation to the S1 and S2 States Studied by 3d-REMPI
32
33 Spectroscopy. *J. Phys. Chem. A* **2010**, *114*, 9948-9962.
34
35

36 (11) Timerghazin, Q. K.; Talipov, M. R. Unprecedented External Electric
37
38 Field Effects on S-Nitrosothiols: Possible Mechanism of Biological Regulation? *J.*
39
40 *Phys. Chem. Lett.* **2013**, *4*, 1034-1038.
41
42

43 (12) Lanucara, F.; Chiavarino, B.; Crestoni, M. E.; Scuderi, D.; Sinha, R. K.;
44
45 Maître, P.; Fornarini, S. S-nitrosation of Cysteine as Evidenced by IRMPD
46
47 Spectroscopy. *Int. J. Mass Spectrom.* **2012**, *330-332*, 160-167.
48

49 (13) Timerghazin, Q. K.; Peslherbe, G. H.; English, A. M. Structure and
50
51 Stability of HSNO, the Simplest S-nitrosothiol. *Phys. Chem. Chem. Phys.* **2008**, *10*,
52
53 1532-1539.
54
55

1
2
3 (14) Fernández-González, M. Á.; Marazzi, M.; López-Delgado, A.; Zapata,
4 F.; García-Iriepa, C.; Rivero, D.; Castaño, O.; Temprado, M.; Frutos, L. M. Structural
5 Substituent Effect in the Excitation Energy of a Chromophore: Quantitative
6 Determination and Application to S-Nitrosothiols. *J. Chem. Theory Comput.* **2012**, *8*,
7 3293-3302.
8

9
10
11
12
13
14 (15) Field, L.; Dilts, R. V.; Ravichandran, R.; Lenhert, P. G.; Carnahan, G. E.
15 An Unusually Stable Thionitrite from N-Acetyl-D,L-penicillamine; X-ray Crystal and
16 Molecular Structure of 2-(Acetylamino)-2-carboxy-1,1-Dimethylethyl Thionitrite. *J.*
17 *Chem. Soc., Chem. Commun.* **1978**, 249-250.
18

19
20
21
22
23 (16) Carnahan, G. E.; Lenhert, P. G.; Ravichandran, R. S-Nitroso-N-acetyl-dl-
24 penicillamine. *Acta Crystallogr.* **1978**, *B34*, 2645-2648.
25

26
27 (17) Arulsamy, N.; Bohle, D. S.; Butt, J. A.; Irvine, G. J.; Jordan, P. A.;
28 Sagan, E. Interrelationships between Conformational Dynamics and the Redox
29 Chemistry of S-Nitrosothiols. *J. Am. Chem. Soc.* **1999**, *121*, 7115-7123.
30
31

32
33 (18) Bartberger, M. D.; Houk, K. N.; Powell, S. C.; Mannion, J. D.; Lo, K. Y.;
34 Stamler, J. S.; Toone, E. J. Theory, Spectroscopy, and Crystallographic Analysis of S-
35 Nitrosothiols: Conformational Distribution Dictates Spectroscopic Behavior. *J. Am.*
36 *Chem. Soc.* **2000**, *122*, 5889-5890.
37
38

39
40 (19) Yi, J.; Khan, M. A.; Lee, J.; Richter-Addo, G. B. The Solid-State
41 Molecular Structure of the S-nitroso Derivative of L-Cysteine Ethyl Ester
42 Hydrochloride. *Nitric Oxide* **2005**, *12*, 261-266.
43
44

45
46 (20) Goto, K.; Hino, Y.; Kawashima, T.; Kaminaga, M.; Yano, E.;
47 Yamamoto, G.; Takagi, N.; Nagase, S. Synthesis and Crystal Structure of a Stable S-
48 nitrosothiol Bearing a Novel Steric Protection Group and of the Corresponding S-
49 nitrothiol. *Tetrahedron Lett.* **2000**, *41*, 8479-8483.
50
51
52
53
54
55
56
57
58
59
60

1
2
3 (21) Perissinotti, L. L.; Estrin, D. A.; Leitus, G.; Doctorovich, F. A
4
5 Surprisingly Stable S-Nitrosothiol Complex. *J. Am. Chem. Soc.* **2006**, *128*, 2512-2513.
6

7 (22) Marazzi, M.; López-Delgado, A.; Fernández-González, M. A.; Castaño,
8
9 O.; Frutos, L. M.; Temprado, M. Modulating Nitric Oxide Release by S-Nitrosothiol
10
11 Photocleavage: Mechanism and Substituent Effects. *J. Phys. Chem. A* **2012**, *116*, 7039-
12
13 7049.
14

15 (23) Romano, R. M.; Della Védova, C. O.; Boese, R. A Solid State Study of
16
17 the Configuration and Conformation of O=S=N-R (R=C₆H₅ and C₆H₃(CH₃-CH₂)₂-2,6).
18
19 *J. Mol. Struct.* **1999**, *475*, 1-4.
20

21 (24) Timerghazin, Q. K.; English, A. M.; Peslherbe, G. H. On the
22
23 Multireference Character of S-nitrosothiols: A -Theoretical Study of HSNO. *Chem.*
24
25 *Phys. Lett.* **2008**, *454*, 24-29.
26
27

28 (25) Hochlaf, M.; Linguerri, R.; Francisco, J. S. On the Role of the Simplest
29
30 S-nitrosothiol, HSNO, in Atmospheric and Biological Processes. *J. Chem. Phys.* **2013**,
31
32 *139*, 234304-234308.
33
34

35 (26) Philippe, R. J. The Infrared Spectrum of Methyl Thionitrite. *J. Mol.*
36
37 *Spectrosc.* **1961**, *6*, 492-496.
38

39 (27) Byler, D. M.; Susi, H. Vibrational Spectra and Normal Coordinate
40
41 Analysis of Methyl Thionitrite and Isotopic Analogs. *J. Mol. Struct.* **1981**, *77*, 25-36.
42
43

44 (28) Niki, H.; Maker, P. D.; Savage, C. M.; Breitenbach, L. P. Spectroscopic
45
46 and Photochemical Properties of Methyl Thionitrite (CH₃SNO). *J. Phys. Chem.* **1983**,
47
48 *87*, 7-9.
49

50 (29) Christensen, D. H.; Rastrup-Andersen, N.; Jones, D.; Klabof, P.;
51
52 Lippincott, E. R. Infrared, Raman and Proton Magnetic Resonance Spectra of
53
54 Methylthionitrite. *Spectrochim. Acta* **1968**, *A24*, 1581-1589.
55
56
57
58
59
60

1
2
3 (30) Mueller, R. P.; Huber, J. R. Two Rotational Isomers of Methyl
4
5 Thionitrite: Light-Induced, Reversible Isomerization in an Argon Matrix. *J. Phys.*
6
7 *Chem.* **1984**, *88*, 1605-1608.

8
9
10 (31) Kennedy, G. R.; Ning, C. L.; Pfab, J. The 355 nm Photodissociation of
11
12 Jet-Cooled CH₃SNO: Alignment of the NO Photofragment. *Chem. Phys. Lett.* **1998**,
13
14 *292*, 161-166.

15
16 (32) Banus, J. Perfluoroalkyl Nitroso Compounds. *Nature* **1953**, *171*, 173-
17
18 174.

19
20 (33) Singh, R. P.; Shreeve, J. M. Perfluoroalkylation of Simple Inorganic
21
22 Molecules: A One Step Route to Novel Perfluoroalkylated Compounds. *Chem. Comm.*
23
24 **2002**, 1818-1819.

25
26 (34) Mason, J. B. Trifluoromethyl Thionitrite. *J. Chem. Soc. (A)* **1969**, 1587-
27
28 1592.

29
30 (35) Kirsch, P.; Bremer, M. Understanding Fluorine Effects in Liquid
31
32 Crystals. *ChemPhysChem* **2010**, *11*, 357-360.

33
34 (36) Oae, S.; Kim, Y. H.; Fukushima, D.; Shinham, K. New Syntheses of
35
36 Thionitrites and their Chemical Reactivities. *J. Chem. Soc. Perkin Trans. 1* **1978**, 913-
37
38 917.

39
40 (37) Philippe, R. J.; Moore, H. The Infrared Spectra of Some Alkyl
41
42 Thionitrites. *Spectrochimica Acta* **1961**, *17*, 1004-1015.

43
44 (38) Tilden, W. A. XXXII.-On Aqua Regia and the Nitrosyl Chlorides. *J.*
45
46 *Chem. Soc.* **1874**, *27*, 630-636.

47
48 (39) Roy, B.; du Moulinet d'Hardemare, A.; Fontecave, M. New Thionitrites:
49
50 Synthesis, Stability, and Nitric Oxide Generation. *J. Org. Chem.* **1994**, *59*, 7019-7026.
51
52
53
54
55
56
57
58
59
60

1
2
3 (40) Hibbert, T. G.; Mahon, M. F.; Molloy, K. C.; Price, L. S.; Parkin, I. P.
4
5 Deposition of Tin Sulfide Thin Films From Novel, Volatile (Fluoroalkylthiolato)tin(IV)
6
7 Precursors. *J. Mat. Chem.* **2001**, *11*, 469-473.
8

9
10 (41) Frisch, M. J.; Trucks, G. W.; Schlegel, H. B.; Scuseria, G. E.; Robb, M.
11
12 A.; Cheeseman, J. R.; Montgomery Jr., J. A.; Vreven, T.; Kudin, K. N.; Burant, J. C.; *et*
13
14 *al.* Gaussian 03; Revision B.04 ed.; Gaussian, Inc.: Pittsburgh PA, 2003.
15

16 (42) Perdew, J. P. Density-Functional Approximation for the Correlation
17
18 Energy of the Inhomogeneous Electron Gas. *Phys. Rev. B* **1986**, *33*, 8822-8824.
19

20 (43) Lee, C.; Yang, W.; Parr, R. G. Development of the Colle-Salvetti
21
22 Correlation-Energy Formula into a Functional of the Electron Density. *Phys. Rev. B*
23
24 **1988**, *37*, 785-789.
25

26 (44) Becke, A. D. Density-Functional Thermochemistry. III. The Role of
27
28 Exact Exchange. *J. Chem. Phys.* **1993**, *98*, 5648-5652.
29

30 (45) Hedberg, L.; Mills, I. M. Harmonic Force Fields from Scaled SCF
31
32 Calculations: Program ASYM40. *J. Mol. Spectrosc.* **2000**, *203*, 82-95.
33

34 (46) Baciu, C.; Gault, J. W. An Assessment of Theoretical Methods for the
35
36 Calculation of Accurate Structures and SN Bond Dissociation Energies of S-
37
38 Nitrosothiols (RSNOs). *J. Phys. Chem. A* **2003**, *107*, 9946-9952.
39

40 (47) Fu, Y.; Mou, Y.; Lin; Liu, L.; Guo, Q.-X. Structures of the X-NO
41
42 Molecules and Homolytic Dissociation Energies of the Y-NO Bonds (Y = C, N, O, S).
43
44 *J. Phys. Chem. A* **2002**, *106*, 12386-12392.
45

46 (48) Erben, M. F.; Della Védova, C. O.; Romano, R. M.; Boese, R.;
47
48 Oberhammer, H.; Willner, H.; Sala, O. Anomeric and Mesomeric Effects in
49
50 Methoxycarbonylsulfonyl Chloride, CH₃OC(O)SOCl: An Experimental and Theoretical
51
52 Study. *Inorg. Chem.* **2002**, *41*, 1064-1071.
53
54
55
56
57
58
59
60

1
2
3 (49) Pasinszki, T.; Vass, G. b.; Klapstein, D.; Westwood, N. P. C. Generation,
4 Spectroscopy, and Structure of Cyanoformyl Chloride and Cyanoformyl Bromide,
5 XC(O)CN. *J. Phys. Chem. A* **2012**, *116*, 3396-3403.
6
7

8
9 (50) Erben, M. F.; Della Védova, C. O.; Boese, R.; Willner, H.; Oberhammer,
10 H. Trifluoromethyl Chloroformate, ClC(O)OCF₃: Structure, Conformation, and
11 Vibrational Analysis Studied by Experimental and Theoretical Methods. *J. Phys. Chem.*
12 *A* **2004**, *108*, 699-706.
13
14
15

16
17 (51) Seth-Paul, W. A. Classical and Modern Procedures for Calculating PR
18 Separations of Symmetrical and Asymmetrical Top Molecules. *J. Mol. Struct.* **1969**, *3*,
19 403-417.
20
21
22
23
24
25
26
27
28
29
30
31
32
33
34
35
36
37
38
39
40
41
42
43
44
45
46
47
48
49
50
51
52
53
54
55
56
57
58
59
60

TOC Graphic

